






Non-conservation of Lepton Numbers in the Neutrino Sector Could Change the Prospects for Core Collapse Supernova Explosions

Anna M. Suliga ^{1,2,3,*} Patrick Chi-Kit Cheong (張志杰) ^{1,4,†} Julien Froustey ^{1,3,5,‡} George M. Fuller ^{3,§} Lukáš Gráf ^{1,3,6,7,¶} Kyle Kehrer ^{3,**} Oliver Scholer ^{8,††} and Shashank Shalgar ^{9,‡‡}

¹Department of Physics, University of California Berkeley, Berkeley, California 94720, USA

²Department of Physics, University of Wisconsin–Madison, Madison, Wisconsin 53706, USA

³Department of Physics, University of California, San Diego, La Jolla, CA 92093-0319, USA

⁴Department of Physics & Astronomy, University of New Hampshire, 9 Library Way, Durham NH 03824, USA

⁵Department of Physics, North Carolina State University, Raleigh, North Carolina 27695, USA

⁶Nikhef, Theory Group, Science Park 105, 1098 XG Amsterdam, The Netherlands

⁷Institute of Particle and Nuclear Physics, Faculty of Mathematics and Physics, Charles University in Prague, V Holešovičkách 2, 180 00 Praha 8, Czech Republic

⁸Max-Planck-Institut für Kernphysik, Saupfercheckweg 1, 69117 Heidelberg, Germany

⁹Niels Bohr International Academy and DARK, Niels Bohr Institute, University of Copenhagen, Blegdamsvej 17, 2100, Copenhagen, Denmark

(Dated: October 1, 2024)

We show that strong interactions violating the conservation of lepton numbers in the neutrino sector could significantly alter the standard low entropy picture for the pre-supernova collapsing core of a massive star. A rapid neutrino-antineutrino equilibration leads to entropy generation and enhanced electron capture and, hence, a lower electron fraction than in the standard model. This would affect the downstream core evolution, the prospects for a supernova explosion, and the emergent neutrino signal. If realized by lepton-number-violating neutrino self-interactions (LNV ν SI), the relevant mediator mass and coupling ranges can be probed by future accelerator-based experiments.

Introduction.— Core collapse supernovae (CCSN) are not only fundamental to our understanding of much of astrophysics and cosmology, but they are in essence weak interaction phenomena and, as such, are alluring venues for studying beyond standard model (BSM) physics, especially in the neutrino sector [1]. In this letter we investigate the effects of lepton number-violating (LNV) physics on the early stages of the collapse of supernova progenitor stars, i.e., those with initial masses in excess of $\sim 10 M_{\odot}$. These stars will suffer prodigious neutrino energy and entropy losses during their short evolutionary time up to the point of core instability and collapse. This entropy loss renders the cores of these stars thermodynamically “cold,” with low entropy-per-baryon, $s_{k_B} \sim 1$ in units of Boltzmann’s constant k_B , with the support pressure dominated by relativistically degenerate electrons. That, in turn, sets up these configurations for instability and collapse. Our study exploits the sensitivity of the subsequent collapse-phase physics to LNV neutrino interactions. This sensitivity arises because such processes can tap into the huge zero point energy reservoir of degenerate electron lepton number ($\sim 10^{57}$) that characterizes the collapsing, pre-bounce core.

The framework for how the weak interaction dictates CCSN core evolution and collapse to a neutron star was confirmed in broad brush by SN1987A [2–4]. The inferred neutrino luminosity was consistent with most of the gravitational binding energy of the proto-neutron star carried off by $\sim 10^{58}$ neutrinos within ~ 10 s [5]. The huge neutrino flux expected from CCSN can serve as a laboratory for neutrino physics [6–16], the vexing prob-

lem of medium-affected nonlinear neutrino flavor oscillations [17–22] and key neutrino mass physics issues [23–25]. The high densities and large electron lepton numbers associated with the CCSN collapse phase preclude neutrino flavor transformation [26], but the downstream post-bounce physics may be affected by these. Nevertheless, the experimental discovery of neutrino oscillations is direct evidence for BSM physics [27–29], spurring proposals for novel experimental and astrophysical probes.

Non-standard neutrino physics could influence neutrino decoupling and Big Bang Nucleosynthesis (BBN) in the early universe. The fossil record of these processes as observed indirectly in the cosmic microwave background (CMB) and cosmic neutrino background ($C\nu B$), e.g., via large scale structure considerations, could provide BSM physics discovery or constraint channels [30–35]. “Secret” neutrino self-interactions (ν SI) as proposed in Ref. [36] have been invoked as a way of coupling the neutrino fluid to itself at the epoch of CMB decoupling, e.g., enabling a potential solution to the Hubble tension problem [37–42]. However, these BSM interactions need not be LNV. The LNV processes we consider may make little difference in a standard, low-lepton-number early universe epoch for neutrino decoupling or BBN [33]. CCSN may provide LNV ν SI insights that are unique or complementary to those gleaned from the early universe. Several works have studied ν SI in CCSN [43–49], including some centered on Majoron-like [50, 51] models [52–60], and others on ν SI-induced alterations of neutrino flavor transformation [61]. The ν SI can also modify the high-energy astrophysical neutrino flux [62–65].

LNV in the Neutrino Sector.— To assess impacts of the lepton-number-violating interactions on collapse let us adopt a ν SI mediated by a scalar field ϕ with

$$\mathcal{L}^\phi = g_{\phi,\alpha\beta} \phi \bar{\nu}_{L,\alpha} \nu_{L,\beta}^c, \quad (1)$$

where in general we can take this interaction to be LNV in one or more neutrino and antineutrino flavors α, β . Here we will consider three ν_e conversion cases that could alter the standard model of stellar collapse: Case (1) $\nu_e \rightleftharpoons \nu_e, \bar{\nu}_e, \nu_\mu, \bar{\nu}_\mu, \nu_\tau, \bar{\nu}_\tau$, Case (2) $\nu_e \rightleftharpoons \nu_e, \bar{\nu}_e, \nu_x, \bar{\nu}_x$, and Case (3) $\nu_e \rightleftharpoons \nu_e, \bar{\nu}_e$. Note that in the heavy mediator limit Case (3) is suppressed for the Lagrangian in Eq. (1) [66, 67]. For Cases (1) and (2), for mediator masses much larger than the momentum exchanged in the interaction, and in the perturbative coupling limit, neutrino-neutrino scattering cross sections can be approximated as [52, 53, 65]

$$\sigma_{\nu\text{SI}} \approx \frac{G_{\nu\text{SI}}^2}{8\pi} E_\nu^{(1)} E_\nu^{(2)} (1 - \cos\theta), \quad (2)$$

where we define the effective neutrino self-coupling $G_{\nu\text{SI}} = g_\phi^2/m_\phi^2$ with g_ϕ and m_ϕ standing for the coupling (assumed to be identical among all flavors) and mass of the new mediator, $E_\nu^{(1,2)}$ being the energies of the interacting neutrinos and $\cos\theta$ denoting the angle between them. For our considerations, the mediator mass must be $m_\phi \gtrsim 100$ MeV to avoid on-shell production during the collapse phase.

Fig. 1 shows the experimental constraints on ν SI and LNV ν SI coupling g_ϕ and mediator mass m_ϕ that stem from meson decay and Z -width measurements [68–71] (1-loop contributions may affect these [72]). The ν SI parameters suggested at CMB decoupling to effect a Hubble tension fix [39] are also shown (green band, upper left), along with parameters that affect or are impacted by CMB considerations (red band) [73]. The LNV ν SI mediator mass and coupling ranges that most affect the collapse epoch are shown as violet shaded regions. The darker of these corresponds to our most conservative estimate of the LNV ν SI strength required for these to dominate over the relevant weak interactions, while the lighter shaded region corresponds to a less stringent, but still plausible, criterion for this. Note that much of the LNV ν SI parameter space relevant for significant collapse epoch effects can be probed by future accelerator-based experiments such as DUNE [71] and Forward Physics Facility (FPF) [74].

Standard core-collapse supernova evolution.—

With Standard Model physics the lead up to collapse of the CCSN core is dominated by neutrino emission-driven entropy loss. At the onset of collapse the core central density is $\rho_{10} \sim 1$ (where $\rho_{10} \equiv \rho/10^{10} \text{ g cm}^{-3}$), the temperature is $T \sim 1$ MeV, and the entropy-per-baryon is $s_{\text{kB}} \sim 1$ [75]. The low entropy implies that the baryonic component is mostly contained in heavy nuclei, with free



FIG. 1. The region of the LNV ν SI parameter space studied in this work together with the terrestrial limits from the Z width and meson decay measurements [68–71], cosmological impacts [39, 73], and projected experimental sensitivities for DUNE [71] and FPF [74]. The dark and light violet shading shows parameters that will alter the standard CCSN collapse physics (see text).

neutrons comprising only $\sim 10\%$ of the total mass fraction, and a much smaller free proton mass fraction, very sensitive to T . The core at this point is already significantly neutronized, with an electron fraction (number of electrons per baryon) of $Y_e \approx 0.4$ [76]. The relativistically degenerate electron component has a Fermi energy $\mu_e \approx 11.1 \text{ MeV} (\rho_{10} Y_e)^{1/3}$. At the onset of collapse this is $\mu_e \approx 7$ MeV. Subsequently, as ρ_{10} and hence μ_e increase during collapse, electron capture on both free protons and those in nuclei will drive Y_e lower. In the early stages of collapse the ν_e produced by electron capture escape the core, so electron capture on free protons lowers the entropy. However, entropy can be increased by electron capture on protons *inside* nuclei because these nuclei can be left in nuclear excited states [75, 77]. When densities in the collapsing core reach $\rho_{10} \approx 10$ to 100, the mean nuclear mass number $\langle A \rangle$ of the nuclei becomes so large that neutrino neutral current coherent scattering [78, 79], with cross section $\sigma_{\nu A} \propto \langle A \rangle^2 E_\nu^2$, leads to neutrinos having mean free paths smaller than the core size, hence they are trapped. Weak (beta) equilibrium is attained quickly thereafter. In beta equilibrium the chemical potentials of all species are related by the Saha equation $\mu_e - \mu_{\nu_e} = \hat{\mu} + \delta m_{np}$, where the ν_e chemical potential is μ_{ν_e} , and $\hat{\mu} = \mu_n - \mu_p$ is the difference of neutron and proton kinetic chemical potentials, and $\delta m_{np} \approx 1.29$ MeV is the neutron-proton mass difference.

In the approach to beta equilibrium, neutrino energies are redistributed not by conservative coherent scattering on nuclei, but rather by neutrino-electron scattering and by neutral current de-excitation of nuclei into neutrino pairs of all flavors [80–85]. The latter process and other thermal neutrino pair creation processes build up zero lepton number populations of ν_μ , $\bar{\nu}_\mu$, ν_τ , $\bar{\nu}_\tau$. Likewise, these create $\bar{\nu}_e$ as well, with the beta equilibrium condition dictating that the Fermi level of $\bar{\nu}_e$ is much lower than that of ν_e . At trapping the overall electron lepton number is $Y_{L_e} = Y_e + Y_{\nu_e} \sim 0.34$, roughly with $Y_e \approx 0.3$ and $Y_{\nu_e} \approx 0.04$, implying a ν_e Fermi level $\mu_{\nu_e} \approx 11.1 \text{ MeV} (2\rho_{10} Y_{\nu_e})^{1/3} \sim 20 \text{ MeV}$.

Subsequent to trapping, as the collapse proceeds, neutrino diffusion out of the core may lower the overall central electron lepton number at core bounce to $\mathcal{O}(0.25)$ [86–93]. Nevertheless, the large degenerate electron lepton number fraction contributes the bulk of the pressure, almost until the central density reaches nuclear density, $\rho_{10} \approx 10^4$. The collapse is abruptly halted at this point, and a shock forms at the edge of the homologous core. The homologous core that serves as a piston for the shock is the inner, causally connected portion of the core inside the sonic point. As the shock moves out through the remainder of the core, the entropy jump $\Delta s_{k_B} \sim 10$ outside the sonic point is sufficient to photo-dissociate the heavy nuclei. This costs $\sim 8 \text{ MeV}$ per nucleon and, consequently, the shock evolves into a standing accretion shock. The shock is later revived by neutrino heating [76] facilitated by hydrodynamic transport [86–89, 91–97].

Core-collapse supernova evolution with νSI .—LNV νSI of sufficient strength would alter this standard picture. In broad brush, at trapping when the neutrino number density rises, the LNV νSI could convert ν_e into neutrinos and antineutrinos of other flavors or types. This could reduce the ν_e Fermi level, altering weak equilibrium by opening phase space for electron capture with many downstream effects. In what follows we present results for Case (1). Results for Cases (2) and (3) are discussed in the Supplemental Material.

For Case (1), $\nu_e \rightleftharpoons \nu_e, \bar{\nu}_e, \nu_\mu, \bar{\nu}_\mu, \nu_\tau, \bar{\nu}_\tau$, all neutrino flavors rapidly thermalize among themselves to a new “neutrino temperature,” T_ν , larger than the matter temperature, T_e . Only the ordinary charged current weak interactions, operating on a longer time scale, can bring the neutrinos and matter back into equilibrium with a common temperature. Re-establishment of equilibrium leads to entropy generation sufficient to shift the nuclear statistical equilibrium (NSE) characterizing the baryonic component from heavy nuclei to, possibly, all free nucleons and alpha particles. The lowering of μ_{ν_e} opens holes for electron capture. This, combined with the larger number of free protons, leads to a precipitous drop in Y_e and, hence, the electron pressure. The net result is that the core will be dominated by non-relativistic pressure.

The key to this radically altered collapse history is

that the νSI be much faster than the weak interactions other than the large coherent neutral current interactions. The latter trap the neutrinos, but have no role in mediating energy exchange between the neutrinos and matter. Therefore, requiring that the νSI interaction mean free path, $\lambda_{\nu\text{SI}}$, be smaller than the core size, R_C , should suffice as a fast νSI criterion. That condition is met when the νSI coupling strength is $G_{\nu\text{SI}} \gtrsim (R_C n_\nu \langle E_\nu \rangle^2 / 8\pi)^{-1/2} \approx 3.6 \times 10^{-4} \text{ GeV}^{-2}$ for the cross section from Eq. (2). The last estimate follows from taking $\lambda_{\nu\text{SI}} \lesssim 10 \text{ km}$ for $E_\nu = 10 \text{ MeV}$ and $Y_{\nu_e} = 0.04$ at density $\rho_{10} = 100$. This is a conservative condition since at trapping $R_C \gg 10 \text{ km}$. This estimate yields a coupling that is not excluded by laboratory experiments (see Fig. 1). For example, Kaon decay experiments provide limits at the level of approximately $G_{\nu\text{SI}} \gtrsim 10^{-2} \text{ GeV}^{-2}$ around $m_\phi \approx 100 \text{ MeV}$ [98].

Evolution toward a new weak equilibrium.—Once the LNV νSI interactions redistribute the ν_e among all neutrino and antineutrino flavors, the core is out of weak equilibrium, and the charged current weak interactions will begin to redistribute energy and lepton number. We can use a Boltzmann equation to follow the evolution toward a new beta equilibrium. We do this calculation with a constant density, $\rho_{10} = 100$, because collapse timescales are relatively long. νSI and electromagnetic interactions, occurring on much shorter timescales than the weak interactions, ensure that all species are in *kinetic* equilibrium and can be described with a temperature T and chemical potential μ . For a given species, the rates of change of the number density dn/dt and of the energy density $d\rho/dt$ imply the following evolution of (T, μ) [99]:

$$\frac{dT}{dt} = \left(\frac{\partial \rho}{\partial \mu} \frac{dn}{dt} - \frac{\partial n}{\partial \mu} \frac{d\rho}{dt} \right) / \left(\frac{\partial n}{\partial T} \frac{\partial \rho}{\partial \mu} - \frac{\partial n}{\partial \mu} \frac{\partial \rho}{\partial T} \right), \quad (3a)$$

$$\frac{d\mu}{dt} = \left(\frac{\partial \rho}{\partial T} \frac{dn}{dt} - \frac{\partial n}{\partial T} \frac{d\rho}{dt} \right) / \left(\frac{\partial n}{\partial \mu} \frac{\partial \rho}{\partial T} - \frac{\partial n}{\partial T} \frac{\partial \rho}{\partial \mu} \right). \quad (3b)$$

We use these to evolve temperatures and chemical potentials for e^- , and all neutrino species. When writing Eq. (3) for electrons, n_{e^-} and ρ_{e^-} change because of weak and QED interactions. Since there are initially almost no positrons, the fast number-changing QED interactions $e^- + e^+ \leftrightarrow \gamma + \gamma$ immediately erase any change in n_{e^+} due to weak interactions. In other words, the net change in e^- number density is $dn_{e^-}/dt = dn_{e^-}/dt|_{\text{weak}} - dn_{e^+}/dt|_{\text{weak}}$, and the same reasoning can be applied to ρ_{e^-} . The evolution equation for e^- quantities is sufficient to describe the whole electromagnetic plasma, since QED interactions ensure $T_{e^-} = T_{e^+} = T_\gamma \equiv T_e$ and $\mu_\gamma = 0$, $\mu_{e^-} = -\mu_{e^+} \equiv \mu_e$.

Figure 2 shows the temporal evolution of the temperatures, matter composition, and pressure. The strong

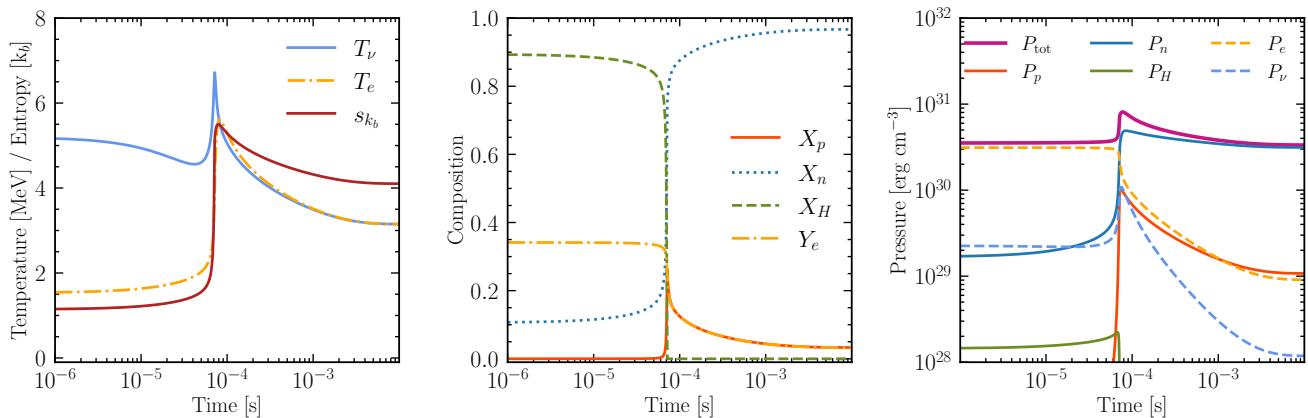


FIG. 2. Temporal evolution of the effective temperatures (in MeV) for neutrinos (T_ν), and the matter component (T_e), and entropy-per-baryon s_{k_B} in units of Boltzmann's constant k_B (*left panel*); the composition of matter: mass fractions for free protons, X_p , free neutrons, X_n , and heavy nuclei, X_H , and electron fraction Y_e (*middle panel*); and the total pressure, P_{tot} , and the pressure contributions for free neutrons and protons, P_n and P_p , respectively, heavy nuclei, P_H , electrons, P_e , and neutrinos of all types, P_ν (*right panel*). We turn on the LNV ν SI at neutrino trapping, Time zero.

LNV ν SI processes equilibrate the $\nu_e, \bar{\nu}_e, \nu_\mu, \bar{\nu}_\mu, \nu_\tau, \bar{\nu}_\tau$ seas, and hence they share a common T_ν and μ_ν whose evolution equations are given in the End Matter. Given our large mediator mass, the relevant ν SI are $2 \rightarrow 2$ processes which conserve the energy and number densities.

Lowering μ_{ν_e} allows enhanced electron capture (see End Matter for the temporal evolution of the weak rates). Figure 2 illustrates the abrupt increase in entropy s_{k_B} that accompanies neutrino equilibration, and the corresponding abrupt decrease in the heavy nucleus mass fraction X_H . The baryonic component is always in NSE and the heavy nucleus mass fraction roughly follows the Saha equation, $X_H \propto s_{k_B}^{1-\langle A \rangle} n_p^Z n_n^N \exp(E_b/T_e)$, where n_p and n_n are, respectively, the overall proton and neutron number densities, and E_b is the binding energy of the nucleus with mass number $\langle A \rangle = N + Z$. As the entropy rises, nuclei with larger $\langle A \rangle$ are disfavored, nearly disappearing when $\Delta s_{k_B} > 3-4$.

In the standard picture of core collapse, the electron pressure, and hence Y_e , determines the size of the homologous core and the initial shock energy after core bounce [77, 100]. With LNV ν SI, Y_e decreases significantly. Higher s_{k_B} and higher matter temperature means a larger free proton mass fraction X_p and that, in turn, favors rapid electron capture with less ν_e blocking. With much higher free neutron mass fraction X_n , and lower Y_e , the pressure will be dominated by the non-relativistic baryonic component.

For Cases (2) and (3), when the ν SI enable LNV among e or e and x neutrino flavors, we obtain core physics alterations that are qualitatively similar to those in Case (1), consistent with results found in Refs. [52, 53].

We point out that the nuclear and weak interaction physics associated with these high entropy conditions has not been explored. Our liquid-drop-based nuclear physics

treatment is likely inadequate (see Supplemental Material). However, we can argue that our results are inevitable for strongly LNV ν SI-coupled ν_e with neutrinos and antineutrinos of multiple flavors that have thermalized with matter and achieved a new beta equilibrium. The only new equilibrium solution is $\mu_{\nu_e} = 0$. Under the assumption that all nuclei melt, and free nucleons are well described by Boltzmann statistics, the new equilibrium values of μ_e and Y_e , for a common temperature T_e , satisfy

$$\mu_e = \delta m_{np} - T_e \ln \left(\frac{Y_e}{1 - Y_e} \right). \quad (4)$$

This can be solved iteratively, with the result that Y_e will be significantly lower and X_n significantly higher (see Fig. 3 in End Matter). Even if the temperature does not increase significantly, the new equilibrium still requires very low Y_e and that likely precludes the existence of a large fraction of heavy nuclei (see Fig. 7 in Supplemental Material).

Discussion and Conclusions.— We have shown that LNV ν SI coupling and mediator mass parameters that are currently unconstrained, but possibly discoverable in future experiments, could drastically alter the CCSN collapse epoch physics. They can do this because they can tap into the huge reservoir of degenerate electron flavor leptons that characterizes the pre-bounce, pre-explosion CCSN.

We point out that a scenario where $2 \rightarrow 4$ processes become important would produce a different evolution in the collapsing core. The lower neutrino energies produced this way could allow neutrinos to escape the infalling core more readily, speeding up the collapse and decreasing Y_e , while leaving the temperature lower. This scenario could lead to a slightly larger heavy nucleus frac-

tion that could persist until a standard nuclear density bounce. The impact of flavor diagonal ν SI $2 \rightarrow 4$ processes has been studied in the context of energy loss arguments for post-bounce evolution in [45].

For LNV ν SI studied in our work, the pressure could be dominated by non-relativistic sources and the temperature will be higher than in the standard case. Is there a thermal bounce [53] before the core reaches nuclear density, or does the collapse proceed to nuclear density, albeit with a larger inner core because of a higher sound speed? Only detailed hydrodynamic and transport simulations with LNV ν SI can answer these questions, but the simulations will have to include the nuclear and weak interaction physics in the exotic high-entropy and low- Y_e conditions found here. However, it is clear that there could be significant alterations in both the emergent neutrino and gravitational wave signals for core collapse with this new physics. For example, the electron neutrino burst expected in the standard CCSN case may be replaced by an electron antineutrino burst originating from positron captures on free neutrons. Such a feature was found in a study of a first-order quark-hadron phase transition during the accretion phase of a CCSN [101] and could have consequences for r-process nucleosynthesis [102].

This unique new physics provides the exciting prospect of synergy and complementarity between very different

experimental probes, from multi-messenger astronomy, including gravitational wave and neutrino detectors, to anticipated accelerator-based laboratory experiments.

Acknowledgments.— We are grateful for helpful discussions with Frank Deppisch, Miguel Escudero, Bronson Messer, Anthony Mezzacappa, Gail McLaughlin, Evan O’Connor, and Sherwood Richers. This work was supported in part by National Science Foundation grant PHY-2209578 at UCSD, and by National Science Foundation grant No. PHY-2020275: *Network for Neutrinos, Nuclear Astrophysics, and Symmetries* (N3AS). Additional support was provided by the Heising-Simons foundation under grant No. 2017-228. This project has received support from the Villum Foundation (Project No. 13164, PI: I. Tamborra), the Danmarks Frie Forskningsfond (Project No. 8049-00038B, PI: I. Tamborra). Further, the work on this project was supported by the Dutch Research Council (NWO), under project number VI.Veni.222.318, and by Charles University through project PRIMUS/24/SCI/013. This research was also supported in part by the INT’s U.S. Department of Energy grant No. DE-FG02-00ER41132 and by the Center for Theoretical Underground Physics and Related Areas (CETUP), The Institute for Underground Science at Sanford Underground Research Facility (SURF), and the South Dakota Science and Technology Authority.

END MATTER

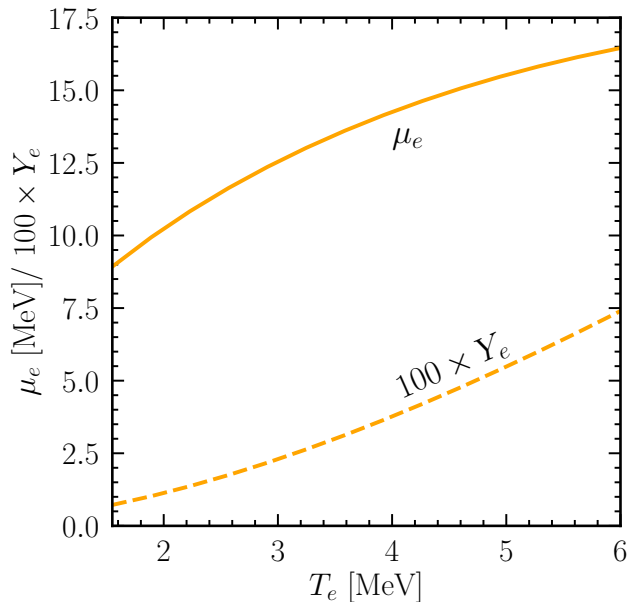


FIG. 3. Solutions for the thermal and chemical equilibrium values of μ_e and Y_e for a given matter temperature T_e and $\mu_{\nu_e} = \mu_{\bar{\nu}_e} = 0$ in the absence of nuclei.

New Weak Equilibrium with LNV ν SI.— Figure 3 shows a solution for a new beta equilibrium with LNV

ν SI (new Y_e and μ_e) with negligible chemical potential for neutrinos and no nuclei present. The solution is the root of Eq. (4). Regardless of the final temperature, the new equilibrium has a significantly lower Y_e .

Weak interaction rates.— We review here an approximate way to calculate the charged-current electron, positron, electron neutrinos and antineutrino capture rates on nucleons and nuclei [77, 103–108].

The charged current emission and absorption processes on nucleons and heavy nuclei determine the change in Y_e during the in-fall phase. This change can be calculated with $dY_e/dt = R_{\nu_e} - R_{\bar{\nu}_e} - R_{e^-} + R_{e^+}$, where the rates per baryon of electron, positron, electron neutrino and antineutrino captures on nuclei and nucleons are

$$R_{\nu_e} = \lambda_{\nu_e}^n X_n + \lambda_{\nu_e}^H (1 - X_n - X_p) / A, \quad (5a)$$

$$R_{\bar{\nu}_e} = \lambda_{\bar{\nu}_e}^p X_p + \lambda_{\bar{\nu}_e}^H (1 - X_n - X_p) / A, \quad (5b)$$

$$R_{e^-} = \lambda_{e^-}^p X_p + \lambda_{e^-}^H (1 - X_n - X_p) / A, \quad (5c)$$

$$R_{e^+} = \lambda_{e^+}^n X_n + \lambda_{e^+}^H (1 - X_n - X_p) / A, \quad (5d)$$

with X_n , X_p and $X_H = 1 - X_n - X_p$ the fractions of free neutrons, free protons, and heavy nuclei in the absence of alpha particles, and

$$\lambda_i^j = \int \sigma_{ij} \frac{dn_i}{dE_i} dE_i = \log 2 \frac{f_{ij}}{ft_{ij}}, \quad (6)$$

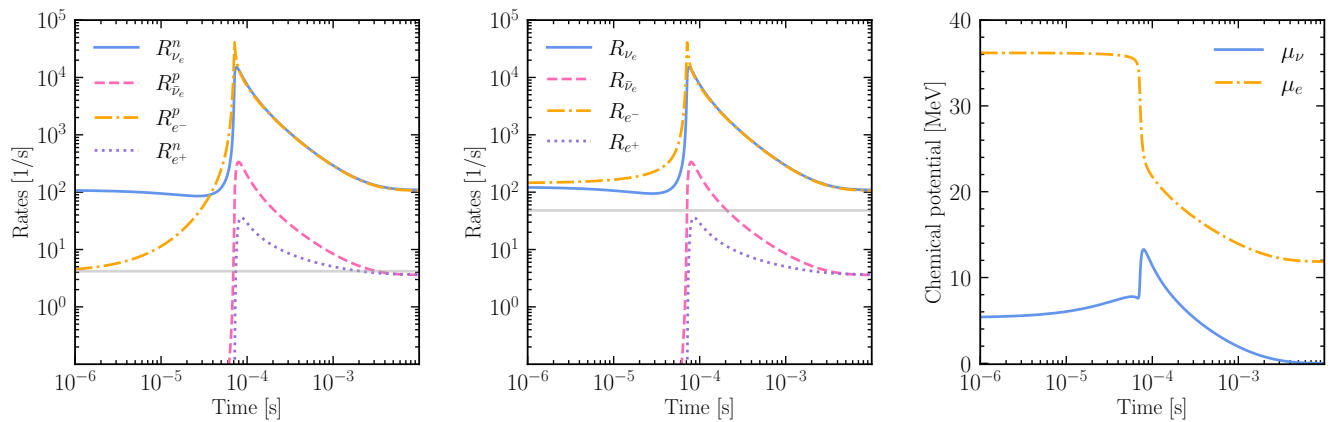


FIG. 4. Temporal evolution of the charged-current weak capture rates of electrons, positrons, electron neutrinos, and electron antineutrinos, and chemical potentials for Case (1). *Left panel*: Captures on free nucleons; *Middle panel*: Total capture rates; *Middle panel*: e^- , ν chemical potentials. Horizontal lines show the electron neutrino and electron capture rates in the SM case. The asymptotic new steady state solution is reached within $\mathcal{O}(1)$ ms.

where σ_{ij} is the cross section for lepton capture between the parent state i and daughter state j , ft_{ij} is the comparative half-life, and the differential particle number density of the relativistic particles l for homogeneous and isotropic distributions is given by $dn_l/dE_l \approx g_l/(2\pi^2)E_l^2 S_l(E_l)$, where l is the statistical weight and S_l is the distribution of particles l over the energy — for fermions in thermal and chemical equilibrium, this is a Fermi-Dirac distribution. The phase space factor f_{ij} for the electron and neutrino captures on the free nucleons and heavy nuclei can be calculated following Ref. [77, 103–105] as

$$f_e^{p,H} = \frac{1}{m_e^5} \int_Q^\infty G E_e^2 (E_e - Q)^2 S_e (1 - S_\nu) dE_e, \quad (7)$$

and

$$f_{\nu_e}^{n,H} = \frac{1}{m_e^5} \int_{E_{\text{th}}}^\infty G E_\nu^2 (Q + E_\nu)^2 S_\nu (1 - S_e) dE_\nu, \quad (8)$$

where S_e and S_ν are the Fermi-Dirac functions for electrons and neutrinos, and G is the Coulomb barrier penetration factor as defined in the Eq. 9 of Ref. [77]. The resonance nuclear Q -value can be approximated with $Q = M_Y - M_X + E_{\text{ex}}$ [77], where M_X (M_Y) is the mass of the parent (daughter) nucleus and E_{ex} is the excitation energy for the Gamow-Teller transition in the daughter nucleus. We use the approximation given in Ref. [105] to calculate the contribution only from the leading transitions such that $Q \approx \hat{\mu} + \delta m_{np} + E_{\text{ex}}$, where $\hat{\mu}$ is the difference between the kinetic chemical potentials of neutrons and protons, but setting $E_{\text{ex}} = 0$. For e^+ and $\bar{\nu}_e$ captures $Q \rightarrow -Q$, the Fermi function and integration thresholds in Eqs. (7) and (8) must be adjusted.

Figure 4 shows the temporal evolution of the charged-current capture rates altered by the presence of the LNV ν SI. The left panel corresponds to the capture rates on

free nucleons, and the right panel corresponds to the total capture rates, i.e., including the captures on free nucleons and nuclei. The increased temperature of the ν_e sea makes ν_e captures on free neutrons and nuclei more efficient, which heats the electrons. Also, the smaller μ_{ν_e} opens up phase space for electron capture on nuclei, increasing the rate for this process. In contrast, e^- capture on free protons is insignificant at the beginning because their small mass fraction is the limiting factor in the overall capture rate. In our simulation, a sufficient amount of entropy to melt the nuclei is generated while attaining the new beta equilibrium; the remaining evolution is dominated by electron captures on free protons.

We have ignored neutrino captures $\nu_e + A(Z-1, N+1) \rightarrow A^*(Z, N) + e^-$ to the highly excited Gamow-Teller resonance state and isobaric analogue state in the daughter nucleus $A^*(Z, N)$ [105]. Though the Gamow-Teller and Fermi strength in these channels is very large, the rate for these channels will be threshold-suppressed and will produce relatively low-energy final state electrons that will tend to be blocked. Moreover, addition of this sub-leading channel would serve only to increase entropy generation, augmenting the evolution towards melting heavy nuclei.

LNV ν SI without Scattering Kernel.— Given the fast equilibration by strong LNV ν SI, the ensemble of (anti)neutrinos is a tightly-coupled fluid for which we can rewrite Eqs. (3a) – (3b) for a common temperature T_ν and a common chemical potential μ_ν . Indeed, the Boltzmann equations read [99]:

$$\sum_\alpha \left(\frac{dn_{\nu_\alpha}}{dt} + \frac{dn_{\bar{\nu}_\alpha}}{dt} \right) = \frac{\delta n_\nu}{\delta t}, \quad (9a)$$

$$\sum_\alpha \left(\frac{d\rho_{\nu_\alpha}}{dt} + \frac{d\rho_{\bar{\nu}_\alpha}}{dt} \right) = \frac{\delta \rho_\nu}{\delta t}, \quad (9b)$$

where α is one of the N_F neutrino flavors and the right-hand sides are the total variation of (anti)neutrino number and energy densities through the charged-current weak interactions. Writing n_ν and ρ_ν the number and energy density of each neutrino species, identical for all species because of ν SI, we can apply the chain rule similarly to Eqs. (3a)–(3b) for all species. The evolution equations for the temperature and chemical potential of

the (anti)neutrino fluid then read

$$\frac{dT_\nu}{dt} = \frac{\frac{\partial \rho_\nu}{\partial \mu_\nu} \frac{\delta n_\nu}{\delta t} - \frac{\partial n_\nu}{\partial \mu_\nu} \frac{\delta \rho_\nu}{\delta t}}{2N_F \left(\frac{\partial n_\nu}{\partial T_\nu} \frac{\partial \rho_\nu}{\partial \mu_\nu} - \frac{\partial n_\nu}{\partial \mu_\nu} \frac{\partial \rho_\nu}{\partial T_\nu} \right)}, \quad (10a)$$

$$\frac{d\mu_\nu}{dt} = \frac{\frac{\partial \rho_\nu}{\partial T_\nu} \frac{\delta n_\nu}{\delta t} - \frac{\partial n_\nu}{\partial T_\nu} \frac{\delta \rho_\nu}{\delta t}}{2N_F \left(\frac{\partial n_\nu}{\partial \mu_\nu} \frac{\partial \rho_\nu}{\partial T_\nu} - \frac{\partial n_\nu}{\partial T_\nu} \frac{\partial \rho_\nu}{\partial \mu_\nu} \right)}. \quad (10b)$$

-
- * asuliga@berkeley.edu
† patrick.cheong@berkeley.edu
‡ jfroustey@berkeley.edu
§ gfuller@physics.ucsd.edu
¶ lukas.graf@nikhef.nl
** kkehrer@ucsd.edu
†† scholar@mpi-hd.mpg.de
‡‡ shashank.shalgar@nbi.ku.dk
- [1] G. G. Raffelt, *Stars as laboratories for fundamental physics: The astrophysics of neutrinos, axions, and other weakly interacting particles* (University of Chicago Press, 1996).
[2] K. Hirata *et al.* (Kamiokande-II), *Phys. Rev. Lett.* **58**, 1490 (1987).
[3] R. M. Bionta *et al.*, *Phys. Rev. Lett.* **58**, 1494 (1987).
[4] E. Alexeyev, L. Alexeyeva, I. Krivosheina, and V. Volchenko, *Phys. Lett. B* **205**, 209 (1988).
[5] A. Burrows and J. M. Lattimer, *Astrophys. J.* **307**, 178 (1986).
[6] G. T. Zatsepin, *Pisma Zh. Eksp. Teor. Fiz.* **8**, 333 (1968).
[7] T. J. Loredo and D. Q. Lamb, *Phys. Rev. D* **65**, 063002 (2002), arXiv:astro-ph/0107260.
[8] G. Pagliaroli, F. Rossi-Torres, and F. Vissani, *Astropart. Phys.* **33**, 287 (2010), arXiv:1002.3349 [hep-ph].
[9] E. Nardi and J. I. Zuluaga, *Phys. Rev. D* **69**, 103002 (2004), arXiv:astro-ph/0306384.
[10] E. Nardi and J. I. Zuluaga, *Nucl. Phys. B* **731**, 140 (2005), arXiv:hep-ph/0412104.
[11] J. F. Beacom, R. N. Boyd, and A. Mezzacappa, *Phys. Rev. Lett.* **85**, 3568 (2000), arXiv:hep-ph/0006015.
[12] J.-S. Lu, J. Cao, Y.-F. Li, and S. Zhou, *JCAP* **05**, 044 (2015), arXiv:1412.7418 [hep-ph].
[13] F. Rossi-Torres, M. M. Guzzo, and E. Kemp, arXiv (2015), arXiv:1501.00456 [hep-ph].
[14] R. S. L. Hansen, M. Lindner, and O. Scholer, *Phys. Rev. D* **101**, 123018 (2020), arXiv:1904.11461 [hep-ph].
[15] F. Pompa, F. Capozzi, O. Mena, and M. Sorel, *Phys. Rev. Lett.* **129**, 121802 (2022), arXiv:2203.00024 [hep-ph].
[16] T. Pitik, D. J. Heimsath, A. M. Suliga, and A. B. Balantekin, *Phys. Rev. D* **106**, 103007 (2022), arXiv:2208.14469 [hep-ph].
[17] H. Duan, G. M. Fuller, and Y.-Z. Qian, *Ann. Rev. Nucl. Part. Sci.* **60**, 569 (2010), arXiv:1001.2799 [hep-ph].
[18] S. Chakraborty, R. Hansen, I. Izaguirre, and G. Raffelt, *Nucl. Phys. B* **908**, 366 (2016), arXiv:1602.02766 [hep-ph].
[19] I. Tamborra and S. Shalgar, *Ann. Rev. Nucl. Part. Sci.* **71**, 165 (2021), arXiv:2011.01948 [astro-ph.HE].
[20] A. V. Patwardhan, M. J. Cervia, and A. B. Balantekin, *Phys. Rev. D* **104**, 123035 (2021), arXiv:2109.08995 [hep-ph].
[21] S. Richers and M. Sen, “Fast Flavor Transformations,” in *Handbook of Nuclear Physics*, edited by I. Tanihata, H. Toki, and T. Kajino (2022) pp. 1–17, arXiv:2207.03561 [astro-ph.HE].
[22] M. C. Volpe, *Rev. Mod. Phys.* **96**, 025004 (2024), arXiv:2301.11814 [hep-ph].
[23] A. S. Dighe and A. Y. Smirnov, *Phys. Rev. D* **62**, 033007 (2000), arXiv:hep-ph/9907423.
[24] M. Aker *et al.* (KATRIN), *Nature Phys.* **18**, 160 (2022), arXiv:2105.08533 [hep-ex].
[25] M. Aker *et al.* (Katrin), (2024), arXiv:2406.13516 [nucl-ex].
[26] G. M. Fuller, R. W. Mayle, J. R. Wilson, and D. N. Schramm, *Astrophys. J.* **322**, 795 (1987).
[27] Y. Fukuda *et al.* (Super-Kamiokande), *Phys. Rev. Lett.* **81**, 1562 (1998), arXiv:hep-ex/9807003.
[28] K. S. Hirata *et al.* (Kamiokande-II), *Phys. Lett. B* **280**, 146 (1992).
[29] A. Bellerive, J. R. Klein, A. B. McDonald, A. J. Noble, and A. W. P. Poon (SNO), *Nucl. Phys. B* **908**, 30 (2016), arXiv:1602.02469 [nucl-ex].
[30] J. F. Beacom, N. F. Bell, and S. Dodelson, *Phys. Rev. Lett.* **93**, 121302 (2004), arXiv:astro-ph/0404585.
[31] N. F. Bell, E. Pierpaoli, and K. Sigurdson, *Phys. Rev. D* **73**, 063523 (2006), arXiv:astro-ph/0511410.
[32] E. Grohs, G. M. Fuller, C. T. Kishimoto, and M. W. Paris, *Phys. Rev. D* **95**, 063503 (2017), arXiv:1612.01986 [astro-ph.CO].
[33] E. Grohs, G. M. Fuller, and M. Sen, *JCAP* **07**, 001 (2020), arXiv:2002.08557 [astro-ph.CO].
[34] J. Froustey and C. Pitrou, *JCAP* **03**, 065 (2022), arXiv:2110.11889 [hep-ph].
[35] J. Froustey and C. Pitrou, (2024), arXiv:2405.06509 [hep-ph].
[36] Z. Bialynicka-Birula, *Nuovo Cim.* **33**, 1484 (1964).
[37] I. M. Oldengott, T. Tram, C. Rampf, and Y. Y. Wong, *JCAP* **11**, 027 (2017), arXiv:1706.02123 [astro-ph.CO].
[38] L. Lancaster, F.-Y. Cyr-Racine, L. Knox, and Z. Pan, *JCAP* **07**, 033 (2017), arXiv:1704.06657 [astro-ph.CO].
[39] M. Park, C. D. Kreisch, J. Dunkley, B. Hadzhiyska, and F.-Y. Cyr-Racine, *Phys. Rev. D* **100**, 063524 (2019),

- arXiv:1904.02625 [astro-ph.CO].
- [40] G. Barenboim, P. B. Denton, and I. M. Oldengott, *Phys. Rev. D* **99**, 083515 (2019), arXiv:1903.02036 [astro-ph.CO].
- [41] N. Blinov, K. J. Kelly, G. Z. Krnjaic, and S. D. McDermott, *Phys. Rev. Lett.* **123**, 191102 (2019), arXiv:1905.02727 [astro-ph.CO].
- [42] G.-y. Huang and W. Rodejohann, *Phys. Rev. D* **103**, 123007 (2021), arXiv:2102.04280 [hep-ph].
- [43] D. A. Dicus, E. W. Kolb, and D. L. Tubbs, *Nucl. Phys. B* **223**, 532 (1983).
- [44] E. W. Kolb and M. S. Turner, *Phys. Rev. D* **36**, 2895 (1987).
- [45] S. Shalgar, I. Tamborra, and M. Bustamante, *Phys. Rev. D* **103**, 123008 (2021), arXiv:1912.09115 [astro-ph.HE].
- [46] S. Reddy and D. Zhou, *Phys. Rev. D* **105**, 023026 (2022), arXiv:2107.06279 [hep-ph].
- [47] P.-W. Chang, I. Esteban, J. F. Beacom, T. A. Thompson, and C. M. Hirata, *Phys. Rev. Lett.* **131**, 071002 (2023), arXiv:2206.12426 [hep-ph].
- [48] D. F. G. Fiorillo, G. G. Raffelt, and E. Vitagliano, *Phys. Rev. D* **109**, 023017 (2024), arXiv:2307.15122 [hep-ph].
- [49] D. F. G. Fiorillo, G. G. Raffelt, and E. Vitagliano, *Phys. Rev. Lett.* **132**, 021002 (2024), arXiv:2307.15115 [hep-ph].
- [50] Y. Chikashige, R. N. Mohapatra, and R. D. Peccei, *Phys. Rev. Lett.* **45**, 1926 (1980).
- [51] G. B. Gelmini and M. Roncadelli, *Phys. Lett. B* **99**, 411 (1981).
- [52] E. W. Kolb, D. L. Tubbs, and D. A. Dicus, *Astrophys. J. Lett.* **255**, L57 (1982).
- [53] G. M. Fuller, R. Mayle, and J. R. Wilson, *Astrophys. J.* **332**, 826 (1988).
- [54] Y. Aharonov, F. T. Avignone, and S. Nussinov, *Phys. Rev. D* **37**, 1360 (1988).
- [55] K. Choi, C. W. Kim, J. Kim, and W. P. Lam, *Phys. Rev. D* **37**, 3225 (1988).
- [56] J. A. Grifols, E. Masso, and S. Peris, *Phys. Lett. B* **215**, 593 (1988).
- [57] R. V. Konoplich and M. Y. Khlopov, *Sov. J. Nucl. Phys.* **47**, 565 (1988).
- [58] Z. G. Berezhiani and A. Y. Smirnov, *Phys. Lett. B* **220**, 279 (1989).
- [59] K. Choi and A. Santamaria, *Phys. Rev. D* **42**, 293 (1990).
- [60] Y. Farzan, *Phys. Rev. D* **67**, 073015 (2003), arXiv:hep-ph/0211375.
- [61] M. Blennow, A. Mirizzi, and P. D. Serpico, *Phys. Rev. D* **78**, 113004 (2008), arXiv:0810.2297 [hep-ph].
- [62] K. C. Y. Ng and J. F. Beacom, *Phys. Rev. D* **90**, 065035 (2014), [Erratum: *Phys. Rev. D* **90**, 089904 (2014)], arXiv:1404.2288 [astro-ph.HE].
- [63] M. Bustamante, C. Rosenström, S. Shalgar, and I. Tamborra, *Phys. Rev. D* **101**, 123024 (2020), arXiv:2001.04994 [astro-ph.HE].
- [64] C. Creque-Sarbinowski, J. Hyde, and M. Kamionkowski, *Phys. Rev. D* **103**, 023527 (2021), arXiv:2005.05332 [hep-ph].
- [65] I. Esteban, S. Pandey, V. Brdar, and J. F. Beacom, *Phys. Rev. D* **104**, 123014 (2021), arXiv:2107.13568 [hep-ph].
- [66] E. E. Jenkins, A. V. Manohar, and P. Stoffer, *JHEP* **03**, 016 (2018), [Erratum: *JHEP* **12**, 043 (2023)], arXiv:1709.04486 [hep-ph].
- [67] R. M. Fonseca and M. Hirsch, *Phys. Rev. D* **98**, 015035 (2018), arXiv:1804.10545 [hep-ph].
- [68] C. Y. Pang, R. H. Hildebrand, G. D. Cable, and R. Stiening, *Phys. Rev. D* **8**, 1989 (1973).
- [69] M. S. Bilenky, S. M. Bilenky, and A. Santamaria, *Phys. Lett. B* **301**, 287 (1993).
- [70] R. Laha, B. Dasgupta, and J. F. Beacom, *Phys. Rev. D* **89**, 093025 (2014), arXiv:1304.3460 [hep-ph].
- [71] J. M. Berryman, A. De Gouvêa, K. J. Kelly, and Y. Zhang, *Phys. Rev. D* **97**, 075030 (2018), arXiv:1802.00009 [hep-ph].
- [72] P. S. B. Dev, D. Kim, D. Sathyan, K. Sinha, and Y. Zhang, (2024), arXiv:2407.12738 [hep-ph].
- [73] M. Archidiacono and S. Hannestad, *JCAP* **07**, 046 (2014), arXiv:1311.3873 [astro-ph.CO].
- [74] K. J. Kelly, F. Kling, D. Tuckler, and Y. Zhang, *Phys. Rev. D* **105**, 075026 (2022), arXiv:2111.05868 [hep-ph].
- [75] H. A. Bethe, G. E. Brown, J. Applegate, and J. M. Lattimer, *Nucl. Phys. A* **324**, 487 (1979).
- [76] H. A. Bethe and J. R. Wilson, *Astrophys. J.* **295**, 14 (1985).
- [77] G. M. Fuller, *Astrophys. J.* **252**, 741 (1982).
- [78] D. Z. Freedman, *Phys. Rev. D* **9**, 1389 (1974).
- [79] D. Akimov *et al.* (COHERENT), *Science* **357**, 1123 (2017), arXiv:1708.01294 [nucl-th].
- [80] G. M. Fuller and B. S. Meyer, *Astrophys. J.* **376**, 701 (1991).
- [81] G. W. Misch, B. A. Brown, and G. M. Fuller, *Phys. Rev. C* **88**, 015807 (2013), arXiv:1301.7042 [astro-ph.HE].
- [82] T. Fischer, K. Langanke, and G. Martínez-Pinedo, *Phys. Rev. C* **88**, 065804 (2013), arXiv:1309.4271 [astro-ph.HE].
- [83] G. W. Misch and G. M. Fuller, *Phys. Rev. C* **94**, 055808 (2016), arXiv:1607.01448 [astro-ph.HE].
- [84] T. Fischer, *Astron. Astrophys.* **593**, A103 (2016), arXiv:1608.05004 [astro-ph.HE].
- [85] A. A. Dzhiyev, A. V. Yudin, N. V. Dunina-Barkovskaya, and A. I. Vdovin, *Mon. Not. Roy. Astron. Soc.* **527**, 7701 (2024), arXiv:2312.07988 [nucl-th].
- [86] H.-T. Janka, *Annual Review of Nuclear and Particle Science* **62**, 407 (2012), arXiv:1206.2503 [astro-ph.SR].
- [87] S. W. Bruenn, A. Mezzacappa, W. R. Hix, E. J. Lentz, O. E. B. Messer, E. J. Lingerfelt, J. M. Blondin, E. Endeve, P. Marronetti, and K. N. Yakunin, *Astrophys. J. Lett.* **767**, L6 (2013), arXiv:1212.1747 [astro-ph.SR].
- [88] S. W. Bruenn *et al.*, *Astrophys. J.* **818**, 123 (2016), arXiv:1409.5779 [astro-ph.SR].
- [89] E. J. Lentz, S. W. Bruenn, W. R. Hix, A. Mezzacappa, O. E. B. Messer, E. Endeve, J. M. Blondin, J. A. Harris, P. Marronetti, and K. N. Yakunin, *Astrophys. J. Lett.* **807**, L31 (2015), arXiv:1505.05110 [astro-ph.SR].
- [90] E. O'Connor *et al.*, *J. Phys. G* **45**, 104001 (2018), arXiv:1806.04175 [astro-ph.HE].
- [91] H. T. Janka, T. Melson, and A. Summa, *Ann. Rev. Nucl. Part. Sci.* **66**, 341 (2016), arXiv:1602.05576 [astro-ph.SR].
- [92] A. Mezzacappa, E. Endeve, O. E. Bronson Messer, and S. W. Bruenn, *Liv. Rev. Comput. Astrophys.* **6**, 4 (2020), arXiv:2010.09013 [astro-ph.HE].
- [93] A. Burrows and D. Vartanyan, *Nature* **589**, 29 (2021), arXiv:2009.14157 [astro-ph.SR].
- [94] S. M. Couch and C. D. Ott, *Astrophys. J.* **799**, 5 (2015),

- arXiv:1408.1399 [astro-ph.HE].
- [95] E. P. O'Connor and S. M. Couch, *Astrophys. J.* **865**, 81 (2018), arXiv:1807.07579 [astro-ph.HE].
 - [96] S. M. Couch and C. D. Ott, *Astrophys. J. Lett.* **778**, L7 (2013), arXiv:1309.2632 [astro-ph.HE].
 - [97] T. Takiwaki, K. Kotake, and Y. Suwa, *Astrophys. J.* **786**, 83 (2014), arXiv:1308.5755 [astro-ph.SR].
 - [98] J. M. Berryman *et al.*, *Phys. Dark Univ.* **42**, 101267 (2023), arXiv:2203.01955 [hep-ph].
 - [99] M. Escudero Abenza, *JCAP* **05**, 048 (2020), arXiv:2001.04466 [hep-ph].
 - [100] G. E. Brown, H. A. Bethe, and G. Baym, *Nucl. Phys. A* **375**, 481 (1982).
 - [101] I. Sagert, T. Fischer, M. Hempel, G. Pagliara, J. Schaffner-Bielich, A. Mezzacappa, F. K. Thielemann, and M. Liebendorfer, *Phys. Rev. Lett.* **102**, 081101 (2009), arXiv:0809.4225 [astro-ph].
 - [102] T. Fischer, M.-R. Wu, B. Wehmeyer, N.-U. F. Bastian, G. Martínez-Pinedo, and F.-K. Thielemann, *Astrophys. J.* **894**, 9 (2020), arXiv:2003.00972 [astro-ph.HE].
 - [103] G. M. Fuller, W. A. Fowler, and M. J. Newman, *Astrophys. J. Suppl.* **142**, 447 (1980).
 - [104] G. M. Fuller, W. A. Fowler, and M. J. Newman, *Astrophys. J. Suppl.* **48**, 279 (1982).
 - [105] G. M. Fuller, W. A. Fowler, and M. J. Newman, *Astrophys. J.* **252**, 715 (1982).
 - [106] K. Langanke, G. Martínez-Pinedo, J. M. Sampaio, D. J. Dean, W. R. Hix, O. E. B. Messer, A. Mezzacappa, M. Liebendorfer, H. T. Janka, and M. Rampp, *Phys. Rev. Lett.* **90**, 241102 (2003), arXiv:astro-ph/0302459.
 - [107] A. Juodagalvis, K. Langanke, W. R. Hix, G. Martínez-Pinedo, and J. M. Sampaio, *Nucl. Phys. A* **848**, 454 (2010), arXiv:0909.0179 [nucl-th].
 - [108] K. Langanke, G. Martínez-Pinedo, and R. Zegers, *Rept. Prog. Phys.* **84**, 066301 (2021), arXiv:2009.01750 [nucl-th].
 - [109] J. M. Lattimer and M. Prakash, *Astrophys. J.* **550**, 426 (2001), arXiv:astro-ph/0002232.
 - [110] S. Hannestad and J. Madsen, *Phys. Rev. D* **52**, 1764 (1995), arXiv:astro-ph/9506015.
 - [111] A. D. Dolgov, S. H. Hansen, and D. V. Semikoz, *Nucl. Phys. B* **503**, 426 (1997), arXiv:hep-ph/9703315.
 - [112] E. Grohs, G. M. Fuller, C. T. Kishimoto, M. W. Paris, and A. Vlasenko, *Phys. Rev. D* **93**, 083522 (2016), arXiv:1512.02205 [astro-ph.CO].
 - [113] J. Froustey, *The Universe at the MeV era: neutrino evolution and cosmological observables*, Ph.D. thesis, Institut d'Astrophysique de Paris, Sorbonne Université, Paris, France (2022), arXiv:2209.06672 [astro-ph.CO].

Supplemental Material for
**Lepton Number Violation in the Neutrino Sector
 Could Change the Prospects for Core Collapse Supernova Explosions**

Anna M. Suliga, Patrick Chi-Kit Cheong, Julien Froustey, George M. Fuller, Lukáš Gráf, Kyle Kehrer,
 Oliver Scholer, and Shashank Shalgar

Here, we provide information that is not necessary to understand the primary message of our work, but that may promote further developments and provide a deeper explanation of some of the points made in the main text.

Lepton Number and Lepton Flavor Violating ν SI for Two and Single Flavor in CCSN

The top panels of Fig. 5 show the temporal evolution of the neutrino and electron temperatures together with the entropy-per-baryon (left panel), the temporal evolution of the matter composition (middle panel), and the pressure (right panel) for the LNV Lepton Flavor Violating (LFV) ν SI with the same coupling for four neutrino species, referred to in the main text as Case (2), whereas the bottom panels illustrate the same quantities for LNV ν SI in Case (3), where only ν_e and $\bar{\nu}_e$ equilibrate by LNV ν SI.

We use the approximation for strong LNV ν SI described in the *End Matter* to evolve only a single temperature T_{ν_e, ν_x} and chemical potential μ_{ν_e, ν_x} for all four neutrinos and antineutrinos in Case (2). The final temperature of the electrons and neutrino fluid is slightly larger than in Case (1), where all of the six (anti)neutrino species participate in LNV ν SI.

For Case (3), we included the LNV ν SI kernels in the evolution equations for ν_e and $\bar{\nu}_e$ temperatures and chemical potentials [Eqs. (3)]. The strong LNV ν SI processes we consider here equilibrate the ν_e and $\bar{\nu}_e$ seas on a very short timescale, and hence T_{ν_e} and $T_{\bar{\nu}_e}$, as well as μ_{ν_e} and $\mu_{\bar{\nu}_e}$. This justifies using a single temperature and chemical potential to evolve those quantities for the strongly coupled by the LNV ν SI neutrino species.

In addition, the matter and neutrinos attain the new weak equilibrium faster in Case (3) than in Cases (1) and (2), because in Case (3) all of the equilibrated by LNV ν SI species of neutrinos can communicate with the matter through charged-current weak interactions.

Partial derivatives of the Fermi Dirac integrals

The evolution equations (3) and (10) require the use of the partial derivatives of the number and energy densities for particles following Fermi-Dirac distributions. These are given by [99]

$$\frac{\partial n}{\partial T} = \frac{g}{2\pi^2} \int dE E \sqrt{E^2 - m^2} \frac{(E - \mu)}{4T^2} \cosh^{-2} \left(\frac{E - \mu}{2T} \right), \quad (11a)$$

$$\frac{\partial \rho}{\partial T} = \frac{g}{2\pi^2} \int dE E^2 \sqrt{E^2 - m^2} \frac{(E - \mu)}{4T^2} \cosh^{-2} \left(\frac{E - \mu}{2T} \right), \quad (11b)$$

$$\frac{\partial n}{\partial \mu} = \frac{g}{2\pi^2} \int dE E \sqrt{E^2 - m^2} \left[2T \cosh \left(\frac{E - \mu}{T} \right) + 2T \right]^{-1}, \quad (11c)$$

$$\frac{\partial \rho}{\partial \mu} = \frac{g}{2\pi^2} \int dE E^2 \sqrt{E^2 - m^2} \left[2T \cosh \left(\frac{E - \mu}{T} \right) + 2T \right]^{-1}, \quad (11d)$$

where the integral limits are (m, ∞) , m is the mass of the fermion, g is the statistical weight, μ is the total chemical potential, T is the temperature, and E is the energy.

Approximate Treatment of the Equation of State

To gather the extent of the effects of altered electron capture rates during the in-fall of the supernova core, we utilize the equation of state (EOS) prescription from Refs. [75, 77]. The equations for the neutron kinetic chemical

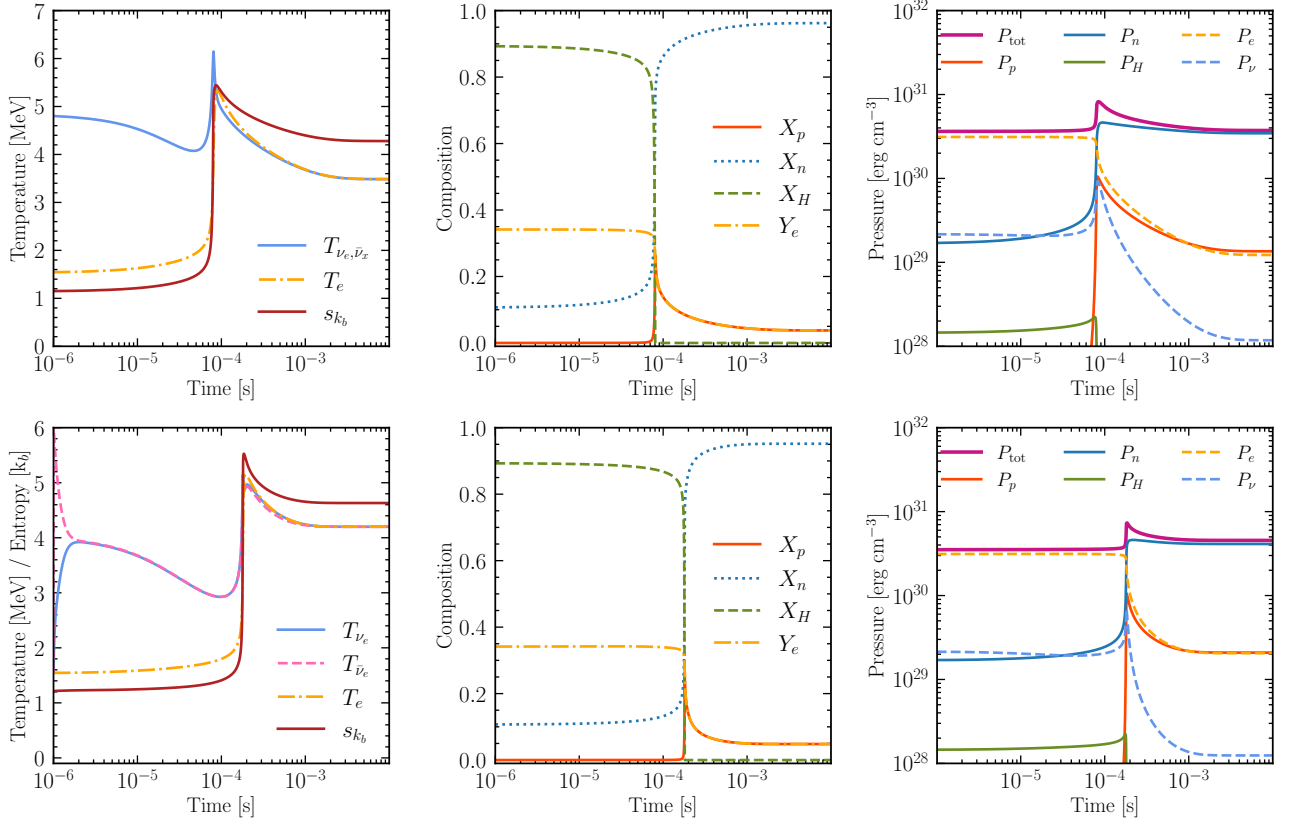


FIG. 5. Temporal evolution of the effective temperatures (in MeV) for neutrinos (T_{ν_i}), and the matter component (T_e), and entropy-per-baryon s_{k_B} in units of Boltzmann's constant k_B (left panel); the composition of matter: mass fractions for free protons, X_p , free neutrons, X_n , and heavy nuclei, X_H , and electron fraction Y_e (middle panel); and the total pressure, P_{tot} , and the pressure contributions for free neutrons and protons, P_n and P_p , respectively, heavy nuclei, P_H , electrons, P_e , and neutrinos of all types, P_ν (right panel). Top panels showcase Case (2) and bottom panels Case (3). We turn on the LNV ν SI at neutrino trapping, Time zero.

potential μ_n , mean nuclear mass $\langle A \rangle$, difference between the neutron and proton kinetic potentials $\hat{\mu}$, and nuclear surface energy are

$$\mu_n = -16 + 125(0.5 - \tilde{Y}_e) - 150(0.5 - \tilde{Y}_e)^2 - 2W_{\text{surf}}\langle A \rangle^{-1/3} \frac{1 - 2\tilde{Y}_e}{1 - \tilde{Y}_e}, \quad (12a)$$

$$\langle A \rangle = \frac{194(1 - \tilde{Y}_e)^2}{1 - 0.236\rho^{1/3}}, \quad (12b)$$

$$\hat{\mu} = 250(0.5 - \tilde{Y}_e) - \frac{W_{\text{surf}}}{\langle A \rangle^{1/3}} \left(\frac{1}{Y_e} + 2\tilde{Y}_e \frac{1 - 2\tilde{Y}_e}{1 - \tilde{Y}_e} \right), \quad (12c)$$

$$W_{\text{surf}} = 290\tilde{Y}_e^2(1 - \tilde{Y}_e)^2. \quad (12d)$$

At low fraction of free protons, the effective electron fraction $\tilde{Y}_e \equiv Z/A \approx Y_e/(1 - X_n)$, however, as the X_p starts to increase, one has to use the full expression $\tilde{Y}_e \equiv Z/A = (Y_e - Y_p)/(1 - X_n - Y_p)$. Once the temperature rises significantly and the electron fraction decreases our EOS prescription may no longer be valid. However, we have checked that the Lattimer and Swesty EOS [109] also restricts the existence of nuclei to approximately 4 MeV for density $\rho_{10} = 100$.

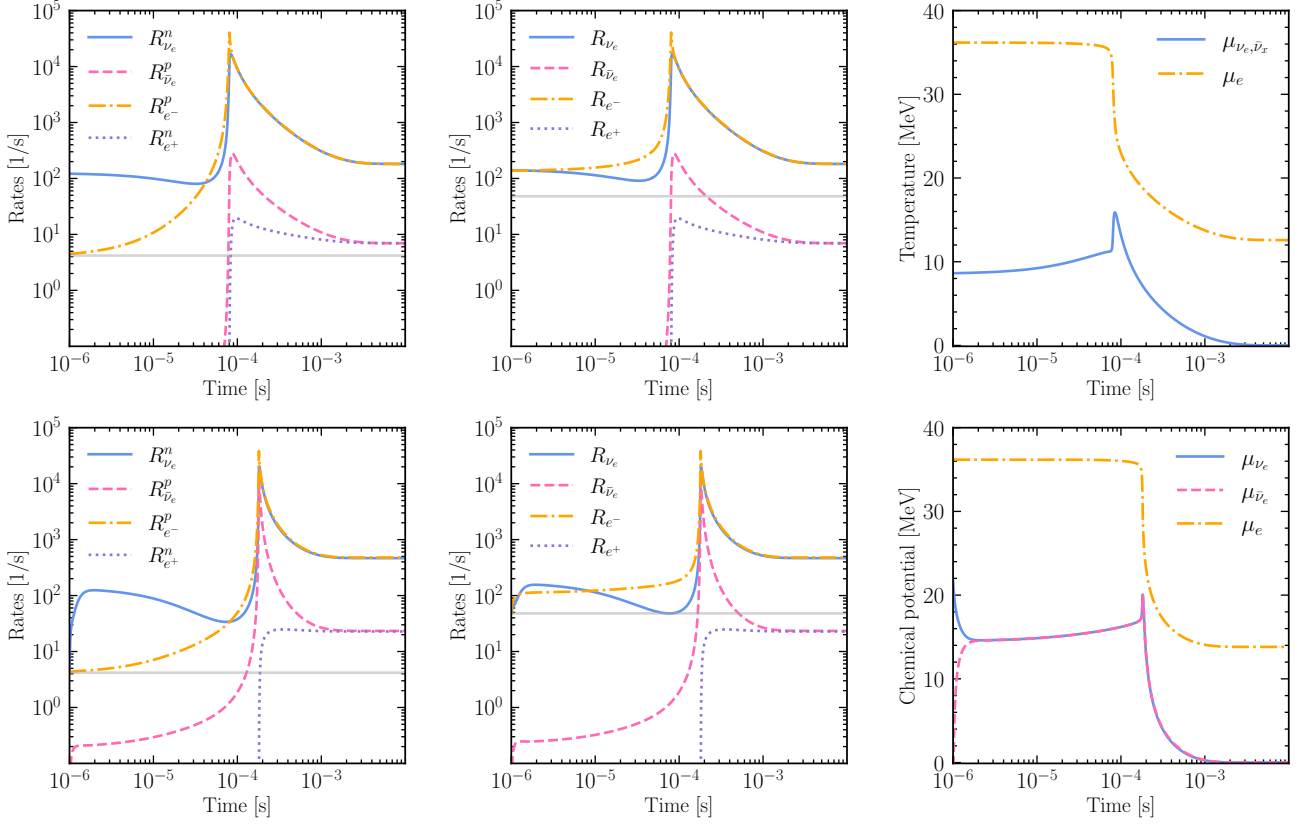


FIG. 6. Temporal evolution of the charged-current weak capture rates of electrons, positrons, electron neutrinos, and electron antineutrinos, and chemical potentials for LNV ν SI between two flavors $\nu_e \rightleftharpoons \nu_e \bar{\nu}_e$, i.e., Case (2) [top panels] and for LNV ν SI in ν_e only, i.e., Case (3) [bottom panels]. Left panel: Captures on free nucleons; Middle panel: Total capture rates; Middle panel: e^- and neutrino chemical potentials. Horizontal lines show the electron neutrino and electron capture rates in the SM case. The asymptotic new steady state solution is reached within $\mathcal{O}(1)$ ms.

ν SI Scattering Kernel

To test the validity of our assumption of treating the several species of neutrinos as a single sea characterized by a single temperature and chemical potential, we modify the evolution equations Eqs. (3) used in Case (3) for both ν_e and $\bar{\nu}_e$ to include the collision terms for the lepton number violating processes $\nu_e + \nu_e \rightleftharpoons \bar{\nu}_e + \bar{\nu}_e$. In general the collision term for two particle scattering inelastically off each other $1 + 2 \rightarrow 3 + 4$ is expressed with [110–113]

$$I_{coll} = \frac{1}{2E_1} \sum \int \frac{d^3 p_2}{2E_2 (2\pi)^3} \frac{d^3 p_3}{2E_3 (2\pi)^3} \frac{d^3 p_4}{2E_4 (2\pi)^3} (2\pi)^4 \delta^{(4)}(p_1 + p_2 - p_3 - p_4) F(S_1, S_2, S_3, S_4) \mathcal{S} \langle |\mathcal{M}|^2 \rangle, \quad (13)$$

where $\langle |\mathcal{M}|^2 \rangle$ is the ν SI LNV interaction matrix element squared and summed over spins of particles 2, 3, 4, the blocking factor is $F = S_3 S_4 (1 - S_1)(1 - S_2) - S_1 S_2 (1 - S_3)(1 - S_4)$, and \mathcal{S} is the symmetrization factor taking care of pairs of identical particles. We have calculated the neutrino-neutrino scattering kernels using the reductions of the nine dimensional integrals to the two dimensional with the use of the integral representation of the delta function [111].

Under the assumption that the CC reactions and electron scattering reactions have timescales much longer than the ν SI we can solve the system of two times number of energy modes differential equations which couple neutrino and antineutrino distributions. The steady state solution for the neutrino and antineutrino distribution is again a Fermi-Dirac distribution that conserves the number of particles and their total energy. The new temperature and chemical potential of neutrinos and antineutrinos, hence, can also be found by solving the energy conservation and

number conservation equations

$$\sum_{\alpha} \int dE E^2 (S_{\nu_{\alpha}}(T_e, \mu_{\nu_{\alpha}}) + S_{\bar{\nu}_{\alpha}}(T_e, \mu_{\bar{\nu}_{\alpha}})) = 2N_F \int dE E^2 S_{\nu_e}(T_{\nu}, \mu_{\nu}), \quad (14a)$$

$$\sum_{\alpha} \int dE E^3 (S_{\nu_{\alpha}}(T_e, \mu_{\nu_{\alpha}}) + S_{\bar{\nu}_{\alpha}}(T_e, \mu_{\bar{\nu}_{\alpha}})) = 2N_F \int dE E^3 S_{\nu_e}(T_{\nu}, \mu_{\nu}). \quad (14b)$$

New Weak Equilibrium with LNV ν SI

We have also solved for the new beta equilibrium $\mu_e = \delta m_{np} + \hat{\mu}$ for our approximate EOS, when the temperature of matter does not heat up too much, and the presence of nuclei is still allowed. Figure 7 shows the solution to the new beta equilibrium with nuclei. The found solution indicates that regardless of the final temperature of matter, the new equilibrium should always have significantly lower Y_e and X_H than in the standard case.

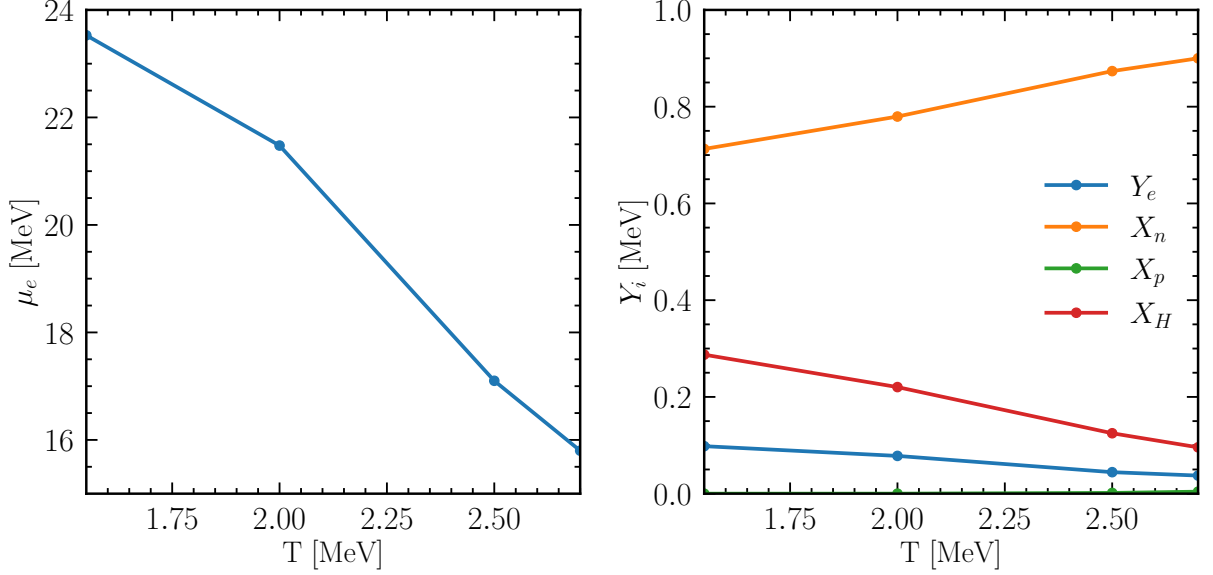


FIG. 7. Solutions for the thermal and chemical equilibrium values of μ_e , Y_e , Y_p , Y_n , X_H for a given temperature of matter T and $\mu_{\nu_e} = \mu_{\bar{\nu}_e} = 0$ in the presence of nuclei for considered in our work approximated EOS prescription.